JACS
JOURNAL OF THE AMERICAN CHEMICAL SOCIETY
pubs.acs.org/JACS
Communication

Divergence and Convergence: Complexity Emerges in Crystal Engineering from an 8-mer DNA

Jiemin Zhao,[⊥] Cuizheng Zhang,[⊥] Brandon Lu, Ruojie Sha, Nicholas Noinaj, and Chengde Mao*

Cite This: J. Am. Chem. Soc. 2023, 145, 10475−10479
Read Online
ACCESS | Metrics & More | Article Recommendations | Supporting Information

ABSTRACT: Biology provides plenty of examples on achieving complicated structures out of minimal numbers of building blocks. In contrast, structural complexity of designed molecular systems is achieved by increasing the numbers of component molecules. In this study, the component DNA strand assembles into a highly complex crystal structure via an unusual path of divergence and convergence. This assembly path suggests a route to minimalists for increasing structural complexity. The original purpose of this study is to engineer DNA crystals with high resolution, which is the primary motivation and a key objective for structural DNA nanotechnology. Despite great efforts in the last 40 years, engineered DNA crystals have not yet consistently reached resolution better than 2.5 Å, limiting their potential uses. Our research has shown that small, symmetrical building blocks generally lead to high resolution crystals. Herein, by following this principle, we report an engineered DNA crystal with unprecedented high resolution (2.17 Å) assembled from one single DNA component: an 8-base-long DNA strand. This system has three unique characteristics: (1) It has a very complex architecture, (2) the same DNA strand forms two different structural motifs, both of which are incorporated into the final crystal, and (3) the component DNA molecule is only an 8-base-long DNA strand, which is, arguably, the smallest DNA motif for DNA nanostructures to date. This high resolution opens the possibility of using these DNA crystals to precisely organize guest molecules at the Å level, which could stimulate a range of new investigations.

Structural complexity and component simplicity are two conflicting parameters in molecular self-assembly. Increasing one usually means sacrificing the other. In a minimalist approach, a question is constantly asked: how can we increase the structural complexity while minimizing the number of component molecules? We present a study on DNA crystal engineering that hints on a potential solution to this question by integrating divergent and convergent assembly. A component DNA strand initially assembles into two different structural motifs that then co-assemble into a DNA crystal.

Structural DNA nanotechnology started in 1982 with a primary goal: to engineer DNA crystals with high resolution so that such DNA crystals could be used to organize guest molecules at the Å level to facilitate the structural study of the guest molecules.[1] Among many efforts,[2−17] a series of DNA crystals was engineered based on a tensegrity triangle motif.[13] This system allowed convenient and systematical variation of the pore size to potentially accommodate different guests.[18] However, the resolutions of such crystals were modest, which prevented the precise organization of guest molecules for structural study. In the course of the study of tensegrity triangle-based DNA crystals, one phenomenon became obvious: small and symmetric motifs resulted in high resolution crystals.[13,19] The same phenomenon was also observed in a DNA crystal system containing parallel DNA duplexes.[20] Herein, following this principle, we have designed an 8-mer DNA (8 nucleotides, nts, long) to assemble into 3D DNA crystals with a resolution of 2.17 Å.

The key to the current design is the spontaneous formation of a symmetric, four-stranded, Holliday junction (HJ) from one unique, 8-mer DNA (AT-CGGCCG), as shown in Figure 1. The DNA sequence contains two palindromes: AT and CGGCCG. It can dimerize into a 6-base pair (bp)-long double-stranded duplex (DS) with two 2-nt-long, self-complementary sticky ends (AT). In addition, this DNA strand contains a G-CC sequence, which has been reported to be able to form a symmetric, four-stranded HJ.[21,22] Therefore, the 8-mer DNAs can potentially homo-tetramerize into a HJ with four sticky ends (AT). The two types of structural motifs (DS and HJ) together could co-assemble along the helical axes through sticky-end cohesion and perpendicular to the helical axes through strand crossovers between adjacent helixes, leading to the formation of 3D crystals.

The crystallization was carried out using a vapor-diffusion method in a hanging-drop setting at 22 °C. After approximately 7 days, sharp-edged crystals over 100 μm appeared (Figure 1d) that diffracted well under X-ray. Its structure was resolved to a resolution of 2.17 Å using molecular replacement with an idealized DNA duplex serving as an initial search model (Supporting Information (SI), Table S1 and Figure S1). This confirmed the design of the engineered DNA crystal. The minimal biological assembly in the crystal comprised of a HJ and a DS, held by sticky-end cohesion (Figure 1e−g). When using a single DNA duplex as a

Received: February 21, 2023
Published: May 3, 2023

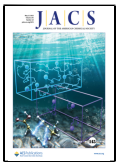

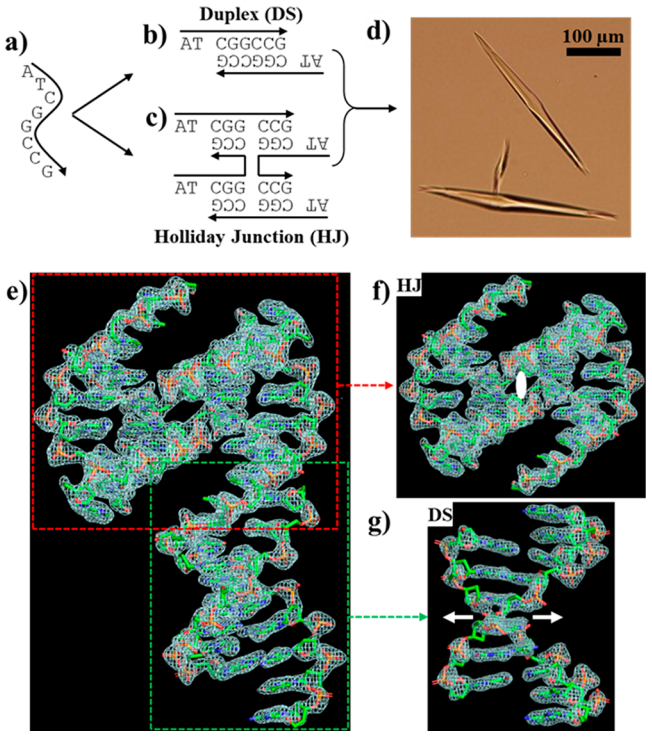

Figure 1. Engineered DNA crystals containing both duplexes (DS) and Holliday junctions (HJ). (a) The single component, 8-mer DNA, which assembles into two different types of motifs: (b) DS and (c) HJ. Both contain the same self-complementary sticky ends and together further assemble into (d) 3D crystals (imaged by optical microscopy). (e) The smallest biological assembly in the crystal as revealed by X-ray crystallography at resolution of 2.17 Å. It contains a (f) HJ and a (g) DS. (e–g) Structural models built into corresponding electron map ($2F_o-F_c$) contoured at 1.5 σ level. 2-fold rotational axes are indicated by a white oval in (f) or a pair of white arrows in (g).

search model, extra electron density was observed in the $2F_o-F_c$ map between two side-by-side, parallel duplexes. This observation prompted us to introduce a pair of strand crossovers to the extra densities (SI, Figure S1c), thereby building a four-stranded HJ (Figure 1f). Both DS and HJ structural models were in good agreement with the electron densities. When increasingly higher contour levels were applied to the electron density map, the remaining, isolated, electron densities located to the phosphate locations, which have the highest densities as phosphorus, is the heaviest atom in the DNA molecule (SI, Figure S2), supporting that the structural model is correct. Please note that each of DS and HJ motifs have a 2-fold rotational axis as indicated in the motif models (Figure 1f,g).

The resulting DNA crystals are chiral and belong to the $H3_2$ space group with cell dimensions as 69.64 Å, 69.64 Å, 72.76 Å, 90.0°, 90.0°, and 120.0° (Figure 2, and SI, Figure S6). They can be viewed as closely packed 2D arrays of interconnected, parallel super-triple helixes that extend infinitely. Such 2D arrays exhibit 3-fold rotational axes along the DNA duplex direction (Figure 2a). The DNA architectures can be described at three different levels.

(i) The basic units as shown in Figure 1e associate with each other by sticky-end cohesion into long, continuous DNA duplexes (Figure 2b, and SI, Figure S3), which swirls into a right-handed, super spirals. At the center of each super spiral, there is a 3-fold screw (3_1) axis. Along the super spiral, the DNA molecules are arranged in HJ–DS–HJ repeats, and the repeats are related to each other by the 3_1 screw axis. Three repeating structural units form a helical turn, which is 3 × 3 × 8 = 72-bp-long along the DNA duplex. A full turn is 217 Å tall. Around the super spiral, HJs are in two groups. In each group, HJs are related to each other by the 3-fold screw axis. The two groups are shifted by 60°. Overall, all HJs are evenly distributed around DNA super spiral in six orientations separated away by 60°.

(ii) Three super DNA spirals wind with each other into a right-handed, super triplex (Figure 2c). At the center of the super triplex, there is a 3-fold rotational axis. One full turn of the super triplex composes of 72 bps and is 217 Å tall. The diameter of the super triplex is 47 Å. Note that the three DNA super spirals in the super triplex have no direct association in terms of hydrogen bonds or strand crossover even though they are in close proximity.

(iii) Each super triplex links its neighboring six super triplexes via strand crossovers of HJs (Figure 2d, and SI, Figures S3 and S4). Any two adjacent super triplexes are linked once every 1/3 of a triplex turn, or 24 bps. Each component super spiral of a super triplex will link with one super spiral from each of the six neighboring super triplexes. With those HJ-mediated linkages, all super triplexes are held together into an interconnected network, forming crystals (SI, Figure S5).

The reported crystal is rationally designed to be assembled from both DS and HJ motifs via sticky-end cohesion. The experimental data have confirmed the main features of the design: the 8-mer DNA forms both DS and HJ motifs, which together co-assemble into the final DNA crystals. However, the high-level, DNA arrangement is a surprise. Figure 3 illustrates the speculated, original design of the DNA crystal, which is fundamentally different from the actual structure we resolved via crystallography. Individual 8-mer DNAs form both DS and HJ motifs (Figure 3a). At this particularly chosen length (8-nt-long), neither type of motif could readily pack in 3D space into crystals. One potential way to form continuous, repetitive 3D lattices is to arrange the two types of motifs alternatingly along any DNA helix direction (Figure 3b, and SI, Figure S6b). In that way, any two adjacent HJ motifs along one helix will be separated by 8 + 8 = 16 bps, or 1.5 helical turns, thus turning 180° and facing to the opposite directions. They will assemble into rhombuses with additional duplexes above and below the rhombus planes. All the duplexes will arrange in three directions, which are sequentially rotated from each other by 120° (the interhelical angle of the HJ) in the *Z*-direction, and then repeat (Figure 3c,d, and SI, Figure S6c,d). Interestingly, the DNA did not completely behave as designed. Instead, the DNA packs much more tightly in the observed crystals. The empty space in the speculated design (82.5%) is far larger than that of the observed crystal (28.1%) (SI, Figure S7). We speculate that such a large difference of occupancy is the primary driving force to form the observed DNA arrangement. Whenever possible, crystals prefer compact packing and avoid empty spaces so that the possibility of unfavorable exposure to free solvent molecules is reduced to maximize overall entropy.[23] That is also the reason for the formation of interpenetrating networks in the literature.[24,25] At the present stage, whether preferring compact packing is general for

https://doi.org/10.1021/jacs.3c01941
J. Am. Chem. Soc. 2023, 145, 10475–10479

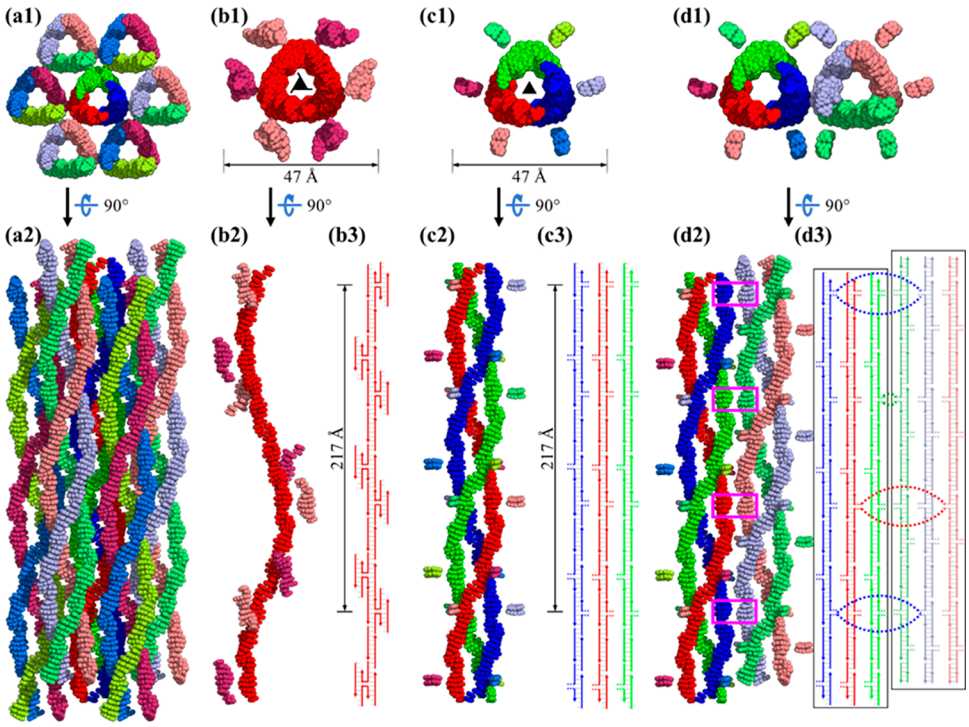

Figure 2. Arrangement of DNA in the crystals. For clarity, only base pairs are shown and backbones are omitted. Neighboring structures may not appear connected due to the omission of the backbones. (a1) and (a2), (b1) and (b2), (c1) and (c2), and (d1) and (d2) are two orthogonal views of the overall DNA arrangement in the DNA crystal, one DNA super spiral, one DNA super triplex, and two interacting DNA super triplexes, respectively. In (b3), (c3), and (d3), corresponding simple schemes of the DNA strand compositions are shown. In (c) and (d), for each HJ, only the two base pairs immediately flanking the junction are shown. Strand crossovers that link the two super triplexes are indicated by purple boxes in (d2) or dash lines in (d3). In the schemes, thick colored lines, thin gray horizontal lines, dashed color lines, and arrows represent DNA backbones, base pairs, strand crossovers, and 3′ ends, respectively. A 3_1-screw axis and a 3-fold rotational axis is shown at the centers in (b1) and (c1), respectively. The size of (b1), (c1), and (d1) is amplified 1.4 times compared with the size of (b2), (c2), and (d2).

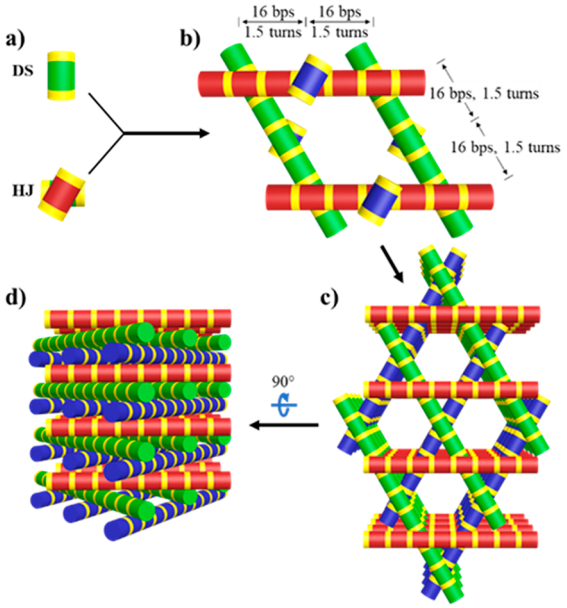

Figure 3. Speculated DNA arrangement in the originally designed DNA crystals. Motifs: DSs and HJs (a), alternatingly associated with each other into rhombuses (b), which further assemble into crystals (c,d), viewed along two orthogonal orientations. Each rod represents a duplex, and golden-colored segments represent sticky ends. Identical HJs are drawn with different colors to make three successive layers with different colors.

engineering DNA crystals is not clear and is worth further studying.

In summary, we have designed an 8-mer DNA to self-assemble into 3D crystals at a resolution of 2.17 Å. This work is significant in several aspects. (i) The component (one 8-mer DNA strand) is arguably the smallest, unique DNA component for assembly of any DNA nanostructure, thus pushing the boundary of the minimalist approach for DNA nanotechnology.[26−28] (ii) The 8-mer DNAs simultaneously form two different structural motifs, and both motifs together assemble into the final crystals. In prior studies, one set of strands always forms only one particular motif under one specific assembly condition;[2−22,29−32] instead, the DNA strands form two different types of motifs in this study, thus leading to higher structural complexity. Such an integration of divergent and convergent assembly is a fundamentally new concept for increasing structural complexity and reducing the number of unique, component DNA strands. (iii) The DNA arrangement in the crystals has the most complicated arrangement in all engineered DNA crystals so far.[2−17,30−32] (iv) The molecular organization is a surprising discovery (though straightforward in retrospective view) that the DNA prefers a compact packing arrangement over a porous packing arrangement. Our findings may provide a strategy for guiding the self-assembly of DNA strands into one particular structure when there are multiple potential structures. In the applied side, the high resolution of the DNA crystals may allow structural studies of small guest molecules that can be incorporated into the DNA crystal lattices,[19] or organize

https://doi.org/10.1021/jacs.3c01941
J. Am. Chem. Soc. 2023, 145, 10475−10479

molecules in 3D with Å level precision for other applications, such as photonic devices,[33] cascade catalysis,[34−36] and information processing and storages.[37−39]

■ ASSOCIATED CONTENT

Supporting Information

The Supporting Information is available free of charge at https://pubs.acs.org/doi/10.1021/jacs.3c01941.

Materials and detailed experimental methods of crystallization and crystallography and figures for additional crystallographic analysis (PDF)

Accession Codes

Crystallography data are available from the Protein Data Bank (https://www.rcsb.org/) with access code 8G4G.

■ AUTHOR INFORMATION

Corresponding Author

Chengde Mao − *Department of Chemistry, Purdue University, West Lafayette, Indiana 47907, United States;* orcid.org/0000-0001-7516-8666; Email: mao@purdue.edu

Authors

Jiemin Zhao − *Institute of Clinical Pharmacology, Key Laboratory of Anti-Inflammatory and Immune Medicine, Ministry of Education, Anhui Collaborative Innovation Center of Anti-Inflammatory and Immune Medicine, Anhui Medical University, Hefei 230032, China; Department of Chemistry, Purdue University, West Lafayette, Indiana 47907, United States;* orcid.org/0000-0002-8939-2156

Cuizheng Zhang − *Department of Chemistry, Purdue University, West Lafayette, Indiana 47907, United States;* orcid.org/0000-0003-3342-7003

Brandon Lu − *Department of Chemistry, New York University, New York, New York 10003, United States;* orcid.org/0000-0001-6424-2197

Ruojie Sha − *Department of Chemistry, New York University, New York, New York 10003, United States*

Nicholas Noinaj − *Department of Biological Sciences, Markey Center for Structural Biology, and the Purdue Institute of Inflammation, Immunology and Infectious Disease, Purdue University, West Lafayette, Indiana 47907, United States;* orcid.org/0000-0001-6361-2336

Complete contact information is available at: https://pubs.acs.org/10.1021/jacs.3c01941

Author Contributions

⊥J.Z. and C.Z. contributed equally to this work.

Notes

The authors declare no competing financial interest.

■ ACKNOWLEDGMENTS

This work was financially supported by NSF (CCF-2107393 and CCMI-2025187 to C.M.), NIH/NIGMS (1R01GM127884 and 1R01GM127896 to N.N.), and the Youth Fund of Anhui Medical University (2022xkj009 to J.Z.). It was also supported by NSF (CCF-2107267 and CCF-2106790).

■ REFERENCES

(1) Seeman, N. C. Nucleic Acid Junctions and Lattices. *J. Theor. Biol.* **1982**, *99*, 237−247.

(2) Simmons, C. R.; Zhang, F.; Birktoft, J. J.; Qi, X.; Han, D.; Liu, Y.; Sha, R.; Abdallah, H. O.; Hernandez, C.; Ohayon, Y. P.; Seeman, N. C.; Yan, H. Construction and Structure Determination of a Three-Dimensional DNA Crystal. *J. Am. Chem. Soc.* **2016**, *138*, 10047−10054.

(3) Simmons, C. R.; Zhang, F.; MacCulloch, T.; Fahmi, N.; Stephanopoulos, N.; Liu, Y.; Seeman, N. C.; Yan, H. Tuning the Cavity Size and Chirality of Self-Assembling 3D DNA Crystals. *J. Am. Chem. Soc.* **2017**, *139*, 11254−11260.

(4) Zhang, F.; Simmons, C. R.; Gates, J.; Liu, Y.; Yan, H. Self-Assembly of a 3D DNA Crystal Structure with Rationally Designed Six-Fold Symmetry. *Angew. Chem. Int. Ed.* **2018**, *57*, 12504−12507.

(5) Simmons, C. R.; MacCulloch, T.; Zhang, F.; Liu, Y.; Stephanopoulos, N.; Yan, H. A Self-Assembled Rhombohedral DNA Crystal Scaffold with Tunable Cavity Sizes and High-Resolution Structural Detail. *Angew. Chem. Int. Ed.* **2020**, *59*, 18619−18626.

(6) Zhao, Y.; Chandrasekaran, A. R.; Rusling, D. A.; Woloszyn, K.; Hao, Y.; Hernandez, C.; Vecchioni, S.; Ohayon, Y. P.; Mao, C.; Seeman, N. C.; Sha, R. The Formation and Displacement of Ordered DNA Triplexes in Self-Assembled Three-Dimensional DNA Crystals. *J. Am. Chem. Soc.* **2023**, *145*, 3599−3605.

(7) Jiang, S.; Zhang, F.; Yan, H. Complex Assemblies and Crystals Guided by DNA. *Nat. Mater.* **2020**, *19*, 694−700.

(8) Simmons, C. R.; MacCulloch, T.; Krepl, M.; Matthies, M.; Buchberger, A.; Crawford, I.; Šponer, J.; Šulc, P.; Stephanopoulos, N.; Yan, H. The Influence of Holliday Junction Sequence and Dynamics on DNA Crystal Self-Assembly. *Nat. Commun.* **2022**, *13*, 3112.

(9) Zhao, Y.; Chandrasekaran, A. R.; Rusling, D. A.; Woloszyn, K.; Hao, Y.; Hernandez, C.; Vecchioni, S.; Ohayon, Y. P.; Mao, C.; Seeman, N. C.; Sha, R. The Formation and Displacement of Ordered DNA Triplexes in Self-Assembled Three-Dimensional DNA Crystals. *J. Am. Chem. Soc.* **2023**, *145*, 3599.

(10) Zhang, T.; Hartl, C.; Frank, K.; Heuer-Jungemann, A.; Fischer, S.; Nickels, P. C.; Nickel, B.; Liedl, T. 3D DNA Origami Crystals. *Adv. Mater.* **2018**, *30*, 1800273.

(11) Stahl, E.; Praetorius, F.; de Oliveira Mann, C. C.; Hopfner, K.-P.; Dietz, H. Impact of Heterogeneity and Lattice Bond Strength on DNA Triangle Crystal Growth. *ACS Nano* **2016**, *10*, 9156−9164.

(12) Zhang, T.; Wei, B. Design of Orthogonal DNA Sticky-End Cohesion Based on Configuration-Specific Molecular Recognition. *J. Am. Chem. Soc.* **2022**, *144*, 18479−18484.

(13) Zheng, J.; Birktoft, J. J.; Chen, Y.; Wang, T.; Sha, R.; Constantinou, P. E.; Ginell, S. L.; Mao, C.; Seeman, N. C. From Molecular to Macroscopic via the Rational Design of a Self-Assembled 3D DNA Crystal. *Nature* **2009**, *461*, 74−77.

(14) Brady, R. A.; Brooks, N. J.; Cicuta, P.; Di Michele, L. Crystallization of Amphiphilic DNA C-Stars. *Nano Lett.* **2017**, *17*, 3276−3281.

(15) Li, Y.; Zhou, W.; Tanriover, I.; Hadibrata, W.; Partridge, B. E.; Lin, H.; Hu, X.; Lee, B.; Liu, J.; Dravid, V. P.; Aydin, K.; Mirkin, C. A. Open-Channel Metal Particle Superlattices. *Nature* **2022**, *611*, 695−701.

(16) Nykypanchuk, D.; Maye, M. M.; van der Lelie, D.; Gang, O. DNA-Guided Crystallization of Colloidal Nanoparticles. *Nature* **2008**, *451*, 549−552.

(17) Yan, X.; Wang, Y.; Ma, N.; Yu, Y.; Dai, L.; Tian, Y. Dynamically Reconfigurable DNA Origami Crystals Driven by a Designated Path Diagram. *J. Am. Chem. Soc.* **2023**, *145*, 3978−3986.

(18) Li, Z.; Liu, L.; Zheng, M.; Zhao, J.; Seeman, N. C.; Mao, C. Making Engineered 3D DNA Crystals Robust. *J. Am. Chem. Soc.* **2019**, *141*, 15850−15855.

(19) Zhang, C.; Zhao, J.; Lu, B.; Seeman, N. C.; Sha, R.; Noinaj, N.; Mao, C. Engineering DNA Crystals toward Studying DNA−Guest Molecule Interactions. *J. Am. Chem. Soc.* **2023**, *145*, 4853−4859.

(20) Paukstelis, P. J.; Nowakowski, J.; Birktoft, J. J.; Seeman, N. C. Crystal Structure of a Continuous Three-Dimensional DNA Lattice. *Chem. Biol.* **2004**, *11*, 1119−1126.

(21) Eichman, B. F.; Vargason, J. M.; Mooers, B. H. M.; Ho, P. S. The Holliday Junction in An Inverted Repeat DNA Sequence:

Sequence Effects on the Structure of Four-Way Junctions. *Proc. Natl. Acad. Sci. U.S.A.* **2000**, *97*, 3971−3976.
(22) Venkadesh, S.; Mandal, P.K.; Gautham, N. The Sequence d(CGGCGGCCGC) Self-Assembles into a Two Dimensional Rhombic DNA Lattice. *Biochem. Biophys. Res. Commun.* **2011**, *407*, 548−551.
(23) Batten, S. R.; Robson, R. Interpenetrating Nets: Ordered, Periodic Entanglement. *Angew. Chem. Int. Ed.* **1998**, *37*, 1460−1494.
(24) Rowsell, J. L. C.; Yaghi, O. M. Effects of Functionalization, Catenation, and Variation of the Metal Oxide and Organic Linking Units on the Low-Pressure Hydrogen Adsorption Properties of Metal-Organic Frameworks. *J. Am. Chem. Soc.* **2006**, *128*, 1304−1315.
(25) Ma, S.; Wang, X.-S.; Yuan, D.; Zhou, H.-C. A Coordinatively Linked Yb Metal−Organic Framework Demonstrates High Thermal Stability and Uncommon Gas-Adsorption Selectivity. *Angew. Chem. Int. Ed.* **2008**, *47*, 4130−4133.
(26) Zuo, H.; Mao, C. A Minimalist's Approach for DNA Nanoconstructions. *Adv. Drug Delivery Rev.* **2019**, *147*, 22−28.
(27) Lau, K. L.; Sleiman, H. F. Minimalist Approach to Complexity: Templating the Assembly of DNA Tile Structures with Sequentially Grown Input Strands. *ACS Nano* **2016**, *10*, 6542−6551.
(28) Fakih, H. H.; Fakhoury, J. J.; Bousmail, D.; Sleiman, H. F. Minimalist Design of a Stimuli-Responsive Spherical Nucleic Acid for Conditional Delivery of Oligonucleotide Therapeutics. *ACS. Appl. Mater. Interfaces* **2019**, *11*, 13912−13920.
(29) He, Y.; Ye, T.; Su, M.; Zhang, C.; Ribbe, A. E.; Jiang, W.; Mao, C. Hierarchical Self-Assembly of DNA into Symmetric Supramolecular Polyhedra. *Nature* **2008**, *452*, 198−201.
(30) Lu, B.; Vecchioni, S.; Ohayon, Y. P.; Sha, R.; Woloszyn, K.; Yang, B.; Mao, C.; Seeman, N. C. 3D Hexagonal Arrangement of DNA Tensegrity Triangles. *ACS Nano* **2021**, *15*, 16788−16793.
(31) Lu, B.; Vecchioni, S.; Ohayon, Y. P.; Woloszyn, K.; Markus, T.; Mao, C.; Seeman, N. C.; Canary, J. W.; Sha, R. Highly Symmetric, Self-Assembling 3D DNA Crystals with Cubic and Trigonal Lattices. *Small* **2023**, *19*, 2205830.
(32) Lu, B.; Woloszyn, K.; Ohayon, Y. P.; Yang, B.; Zhang, C.; Mao, C.; Seeman, N. C.; Vecchioni, S.; Sha, R. Programmable 3D Hexagonal Geometry of DNA Tensegrity Triangles. *Angew. Chem. Int. Ed.* **2023**, *62*, No. e202213451.
(33) Zhou, X.; Satyabola, D.; Liu, H.; Jiang, S.; Qi, X.; Yu, L.; Lin, S.; Liu, Y.; Woodbury, N. W.; Yan, H. Two-Dimensional Excitonic Networks Directed by DNA Templates as an Efficient Model Light-Harvesting and Energy Transfer System. *Angew. Chem. Int. Ed.* **2022**, *61*, No. e202211200.
(34) Delebecque, C. J.; Lindner, A. B.; Silver, P. A.; Aldaye, F. A. Organization of Intracellular Reactions with Rationally Designed RNA Assemblies. *Science* **2011**, *333*, 470−474.
(35) Fu, J.; Liu, M.; Liu, Y.; Woodbury, N. W.; Yan, H. Interenzyme Substrate Diffusion for an Enzyme Cascade Organized on Spatially Addressable DNA Nanostructures. *J. Am. Chem. Soc.* **2012**, *134*, 5516−5519.
(36) Roelfes, G.; Feringa, B. L. DNA-Based Asymmetric Catalysis. *Angew. Chem. Int. Ed.* **2005**, *44*, 3230−3232.
(37) Qian, L.; Winfree, E. Scalilng up digital circuit computation with DNA strand displacement cascades. *Science* **2011**, *332*, 1196−1201.
(38) Ceze, L.; Nivala, J.; Strauss, K. Molecular digital data storage using DNA. *Nat. Rev. Genet.* **2019**, *20*, 456−466.
(39) Mao, C.; Wang, S.; Li, J.; Feng, Z.; Zhang, T.; Wang, R.; Fan, C.; Jiang, Xi. Metal−Organic Frameworks in Microfluidics Enable Fast Encapsulation/Extraction of DNA for Automated and Integrated Data Storage. *ACS Nano* **2023**, *17*, 2840−2850.

https://doi.org/10.1021/jacs.3c01941
J. Am. Chem. Soc. 2023, 145, 10475−10479